

Determining Parastichy Numbers Using Discrete Fourier Transforms

Riichirou Negishi^{1*}, Kumiko Sekiguchi¹, Yuichi Totsuka² and Masaya Uchida¹

¹Saitama Institute of Technology, 1690 Fussaiji, Fukaya, Saitama 369-0293, Japan

²Global Software Co. Ltd., 3-11-10 Kenpuku, Honjo, Saitama 367-0044, Japan

*E-mail address: negishi@sit.ac.jp

(Received September 21, 2017; Accepted October 31, 2017)

We report a practical method to assign parastichy numbers to spiral patterns formed by sunflower seeds and pineapple ramenta using a discrete Fourier transform. We designed various simulation models of sunflower seeds and pineapple ramenta and simulated their point patterns. The parastichy numbers can be directly and accurately assigned using the discrete Fourier transform method to analyze point patterns even when the parastichy numbers contain a divergence angle that results in two or more generalized Fibonacci numbers. The presented method can be applied to extract the structural features of any spiral pattern.

Key words: Parastichy Number, Fibonacci Number, Fourier Transform, Sunflower Seeds, Pineapple Ramenta

1. Introduction

Sunflower florets or seeds are arranged in spirals on the head inflorescence. Spiral arrangements are characterized by the number of spirals going clockwise (CW) and counter-clockwise (CCW), and the spiral number is called the parastichy number. Around the 18th century, Johannes Kepler observed that the Fibonacci numbers are common in plants (Adler *et al.*, 1997). Figure 1 shows the seed pattern in a sunflower head. When the number of spirals toward the outer rim in Fig. 1 is visually counted, the parastichy numbers are assigned to be 21/34, 34/55, and 55/89 (CW or CCW). These numbers correspond to Fibonacci numbers (1, 1, 2, 3, 5, 8, 13, 21, 34, 55, 89, ...). These parastichy numbers have attracted the attention of researchers over many centuries (Vogel, 1979). Sunflower seed spirals were studied by multiple scientists following Hofmeister's (1868) systematic description of a mechanism of phyllotaxis including spiral formation (Adler *et al.*, 1997; Mathai and Davis, 1974). Alan Turing sketched seed patterns and studied Fibonacci phyllotaxis (Turing, 1952; Turing Archive, 1956). Linden (1990) obtained a sunflower-like spiral formation via the dislodgement model without using a divergence angle. Dunlap (1997) emphasized the fundamental properties of Fibonacci numbers and their application to the diverse fields of mathematics, computer science (Negishi and Sekiguchi, 2007), physics, and biology. Such spirals and parastichy numbers have also attracted attention in various model systems including laboratory experiments. For example, Douady and Couder (1992) successfully obtained Fibonacci spirals with drops of ferrofluid under the influence of a magnetic field. Spiral structures are emerging as powerful nanophotonic platforms with distinctive optical properties for multiple engineering applications (Agrawal *et al.*, 2008; Trevino *et al.*, 2008; Negro *et al.*,

2012; Liew *et al.*, 2011). Interestingly, circularly symmetric scattering resonances in aperiodic spirals can carry orbital angular momentum (Trevino *et al.*, 2008).

Adler (1974) proposed a theorem to determine the number sequences for various divergence angles. Jean (2009) summarized the relationship between the divergence angles and the number sequences using Adler's theorem. Table 1 shows the calculated number sequences for various divergence angles using Adler's theorem. In Table 1, the Fibonacci sequence is denoted by F , the Lucas sequence is denoted by L , and the generalized Fibonacci sequences are denoted by G (Koshy, 2001). Two successive numbers can be related as follows:

$$\lim_{n \rightarrow \infty} \frac{G_{n+1}}{G_n} \rightarrow \tau = 1.61803 \dots \quad (1)$$

For a divergence angle of 137.51° , which is approximately equal to the golden angle ϕ_τ ($137.507764 \dots^\circ$), the parastichy numbers reflect the Fibonacci sequence (F). When the divergence angle is 99.50° , the parastichy numbers give the Lucas sequence (L). Generalized Fibonacci sequences (G) appear for divergence angles such as 77.96° and 64.08° .

Spirals with remarkably different structures can be obtained by choosing only slightly different values for the divergence angle. For example, Fig. 2 shows a simulation of the point pattern of a sunflower model with a divergence angle of 137.4° , which is slightly smaller than the golden angle (see details in Sec. 2.1). The parastichy numbers in the outer rim are composed of the Fibonacci number 55 and the Lucas number 76 (hereafter, they are written as $F55$ and $L76$, respectively). In this case, the parastichy numbers cannot be calculated using Adler's theorem. Novel Fibonacci and non-Fibonacci structures in sunflowers have recently been reported in this context (Swinton *et al.*, 2016). Therefore, a practical method to assign parastichy numbers to any spiral pattern is needed.

Vogel (1979) was one of the first researchers to develop a

Table 1. Number sequences for various divergence angles.

Divergence angle	Sequences
137.51°	$F, G(1, 2) : 1, 2, 3, 5, 8, 13, 21, 34, 55, 89, 144, 233, 377, 610, 987, 1597, \dots$
99.50°	$L, G(1, 3) : 1, 3, 4, 7, 11, 18, 29, 47, 76, 123, 199, 322, 521, 843, 1364, \dots$
77.96°	$G(1, 4) : 1, 4, 5, 9, 14, 23, 37, 60, 97, 157, 254, 411, 665, 1076, \dots$
64.08°	$G(1, 5) : 1, 5, 6, 11, 17, 28, 45, 73, 118, 191, 309, 500, 809, 1309, \dots$
54.40°	$G(1, 6) : 1, 6, 7, 13, 20, 33, 53, 86, 139, 225, 364, 589, 953, 1542, \dots$
47.25°	$G(1, 7) : 1, 7, 8, 15, 23, 38, 61, 99, 160, 259, 419, 678, 1097, 1775, \dots$
151.14°	$G(2, 5) : 2, 5, 7, 12, 19, 31, 50, 81, 131, 212, 343, 555, 898, 1453, \dots$
158.15°	$G(2, 7) : 2, 7, 9, 16, 25, 41, 66, 107, 173, 280, 453, 733, 1186, 1919, \dots$

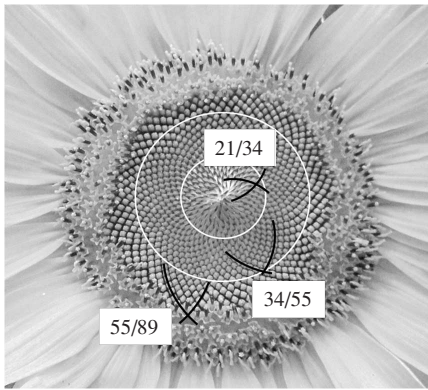


Fig. 1. The seed pattern of a sunflower head displaying Fibonacci numbers. The black and white lines are counting guides marked on the original sunflower.

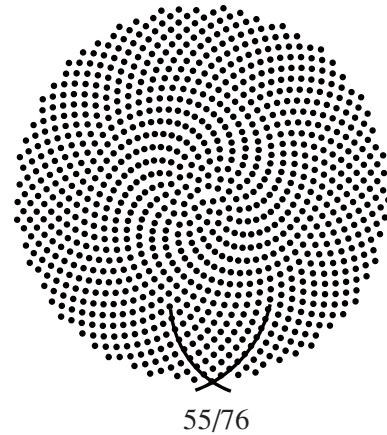


Fig. 2. Simulated point pattern of a sunflower model with a divergence angle of 137.4° and $n = 1000$.

mathematical spiral model to approximate the complex arrangements of the florets in the sunflower head. However, Vogel's spirals lack both translational and orientational symmetry in real space. Accordingly, the Fourier space of Vogel's spirals does not exhibit well-defined Fourier peaks but shows diffuse circular rings, similar to the electron diffraction patterns observed in amorphous solids and liquids (Trevino *et al.*, 2008). This suggests that point distances in a short range are required to analyze spirals. Liew *et al.* (2011) applied the Fourier-Bessel transform to understand the structural complexity of the golden angle spiral. Pennybacker *et al.* (2015) clarified the relationship between parastichy numbers and Fourier decompositions in phyllotactic patterns. We reported a practical method to obtain parastichy numbers using a discrete Fourier transform focusing on the circular symmetry in Fourier space. Fourier transforms are widely used to grasp the characteristics of periodic and aperiodic patterns in natural phenomena and to analyze crystal structures via X-ray diffraction (Authier, 2001; Kikuta, 2011). We tested our method's applicability with sunflower and pineapple models. We applied the discrete Fourier transform to the simulated point patterns of the models. Parastichy numbers for point patterns with various divergence angles were examined in detail.

2. Simulation Models

2.1 Sunflower model

For a sunflower model, the point positions can be determined by the following equation in polar coordinates (r, θ)

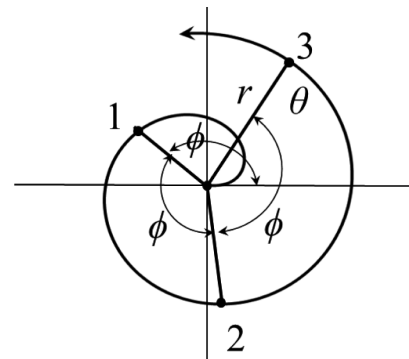


Fig. 3. Spiral trajectory of a sunflower model.

(Fig. 3):

$$(r, \theta) = (n^p, n\phi). \quad (2)$$

Here, n is an integer, p is a constant scaling factor, and ϕ is the divergence angle. When $n = 1000$, $p = 0.5$, and $\phi = \phi_\tau$, the points form the spiral shape shown in Fig. 4. Dominant parastichy numbers can be visually counted toward the outer rim as 21/34, 34/55, and 55/89, which correspond to Fibonacci numbers. The parastichy numbers vary depending on the values of n , p , and ϕ , as we will see later.

2.2 Pineapple model

A pineapple model is expressed by points on the surface of a cylinder, as shown in Fig. 5. The height l and the argu-

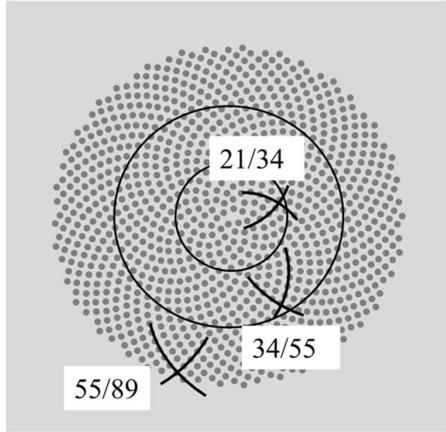


Fig. 4. Simulated point pattern of a sunflower model with $n = 1000$, $p = 0.5$, and $\phi = \phi_\tau$. The black lines are counting guides.

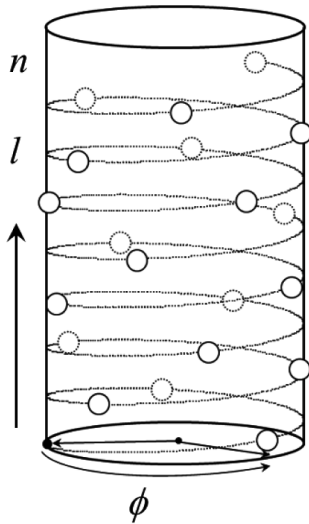


Fig. 5. A pineapple model expressed by points on the surface of a cylinder.

ment angle θ are determined by n , p , and ϕ . Point positions on the cylinder for a pineapple model can be generated via the expression $(l, \theta) = (n^p, n\phi)$. Figure 5 shows point positions with $n = 20$, $p = 1$, and $\phi = \phi_\tau$. Figure 6 is the point pattern developed after the cylinder in Fig. 5 was cut open along the height direction. For $n = 1000$, the points fill a rectangle having a horizontal side of 2π and a vertical side of l . The points form a series of straight lines in Fig. 6. The parastichy numbers around the top of the cylinder were visually counted as 13, 21, 34, and 55, which correspond to Fibonacci numbers. The parastichy numbers of pineapple models also vary depending on the values of n , p , and ϕ .

3. Analysis Procedure Using a Discrete Fourier Transform

3.1 The case of the sunflower model

We presented a method using a discrete Fourier transform to assign parastichy numbers to sunflower models. The overall arrangement of seeds on the sunflower head was a variable spiral structure by the radius position. Therefore, we focused on the short-range arrangement of the

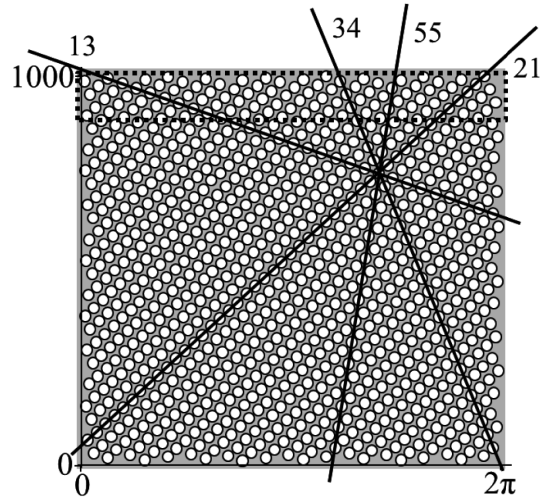


Fig. 6. Simulated developed point pattern of a pineapple model with $n = 1000$, $p = 1$, and $\phi = \phi_\tau$. The dotted rectangle shows a measured area for counting the parastichy numbers.

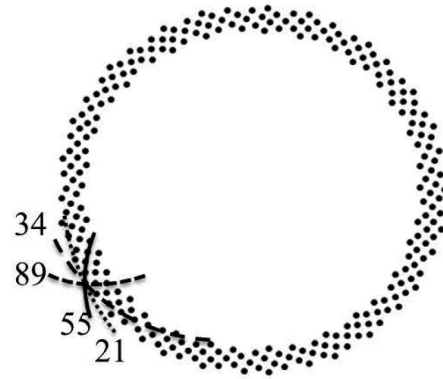


Fig. 7. Simulated point pattern in the outer rim of a sunflower model with $n = 1000$, $p = 0.5$, and $\phi = \phi_\tau$, showing parastichy numbers of 21/34, 34/55, and 55/89.

seeds (points) at a given radius. Figure 7 shows the simulated point pattern in the outer rim of the pattern in Fig. 4 with $n = 1000$, $p = 0.5$, and $\phi = \phi_\tau$. Our assignment method was based on a discrete Fourier transform of the set of distances from each point to the closest point in the spiral pattern. A Fourier transform peak position (spatial frequency) corresponded to a parastichy number. The number of sample points for the discrete Fourier transform was selected to be a power of 2, i.e., 256 points. First, an azimuth angle θ for each point was calculated, and the sample data were arranged in ascending order of their angles. Then, the distance from each point to the closest point with a smaller angle was measured, and a dataset was formed. Using the Wolfram Mathematica software package, a one-dimensional discrete Fourier transform was applied to the dataset. Figure 8 shows the absolute value of the Fourier transform spectra. Due to conjugate symmetry for real sequences, the half data range is shown. The same procedure was applied to the second, third, and fourth closest points. Finally, the Fourier data were summed from the first closest to the fourth closest points to obtain a more accurate power spectrum (Fig. 9).

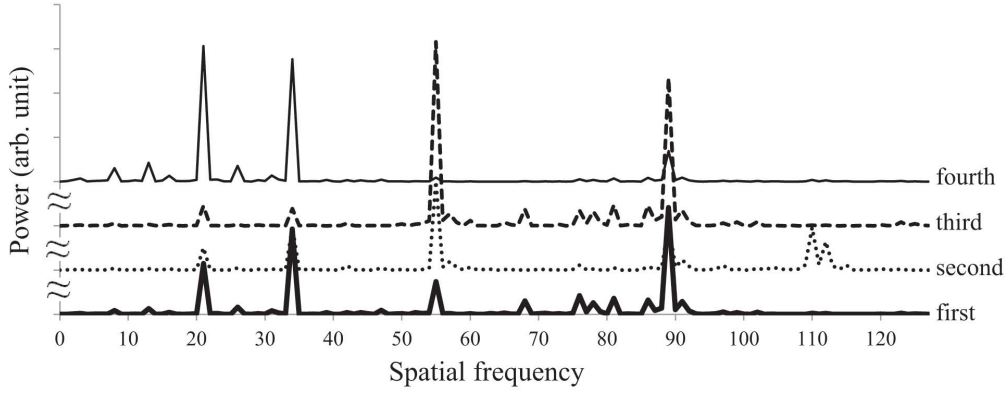


Fig. 8. One-dimensional discrete Fourier transform results for the first, second, third, and fourth closest points in a sunflower model with $n = 1000$, $p = 0.5$, $\phi = \phi_\tau$, and 256 sample points.

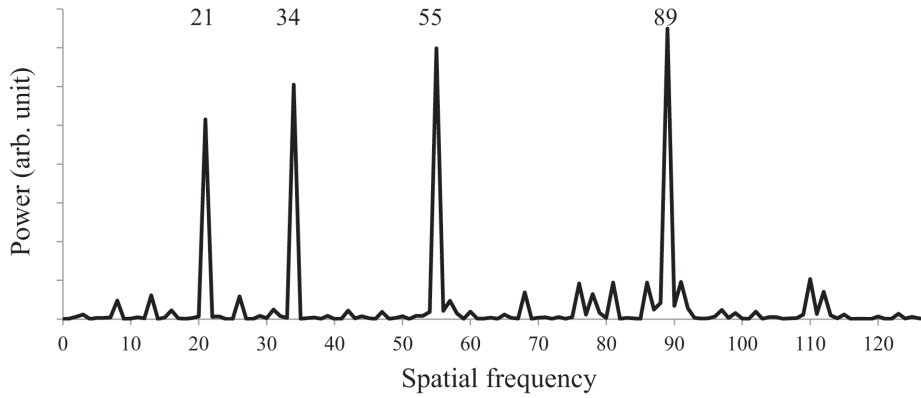


Fig. 9. The Fourier transform result (sum of the data from the first closest points to the fourth closest points in Fig. 8).

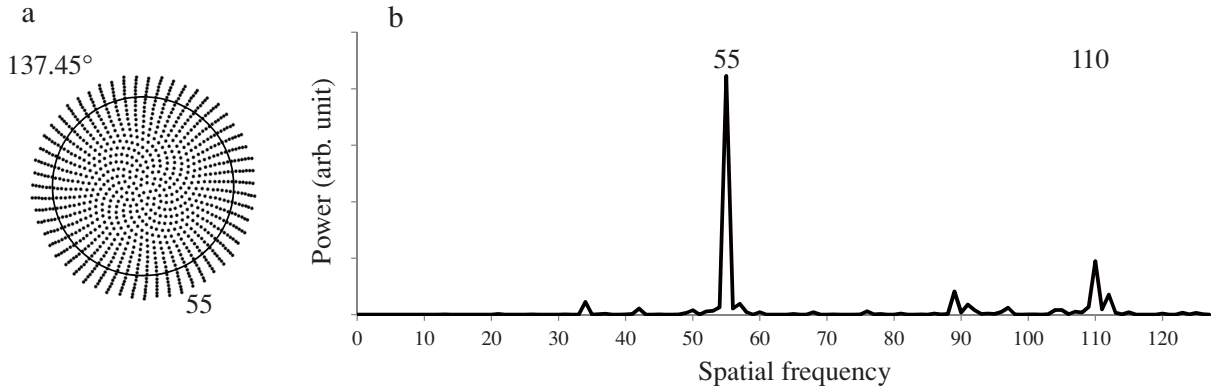


Fig. 10. (a) A simulated point pattern for a sunflower model with $\phi = 137.45^\circ$ and $n = 1000$. (b) The Fourier transform result for the area outside the black circle in panel (a).

In Fig. 9, four large peaks can be seen with spatial frequencies of 21, 34, 55, and 89. These values agreed with the visually counted parastichy numbers in Fig. 7. This agreement indicated that parastichy numbers could be assigned using the presented Fourier transform method.

3.2 The case of the pineapple model

The method for a pineapple model was the same as that for a sunflower model. The number of sample points was 128 points in the dotted rectangle as shown in Fig. 6.

4. Results and Discussion

4.1 Parastichy numbers near the golden angle in sunflower models

Parastichy numbers for the golden angle ϕ_τ in the sunflower model were investigated in Subsec. 3.1 and obtained using the Fourier transform method. Here we investigated parastichy numbers near the golden angle ϕ_τ for the sunflower model. Figure 10(a) is a simulated point pattern for the case of $\phi = 137.45^\circ$, which is slightly smaller than ϕ_τ . Interestingly, the points radiated outward in all direc-

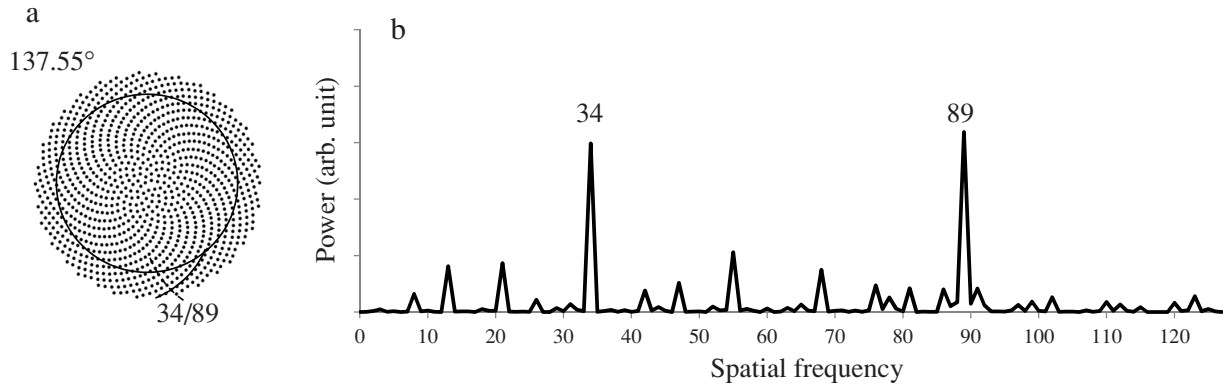


Fig. 11. (a) A simulated point pattern for a sunflower model with $\phi = 137.55^\circ$ and $n = 1000$. (b) The Fourier transform result for the area outside the black circle in panel (a).

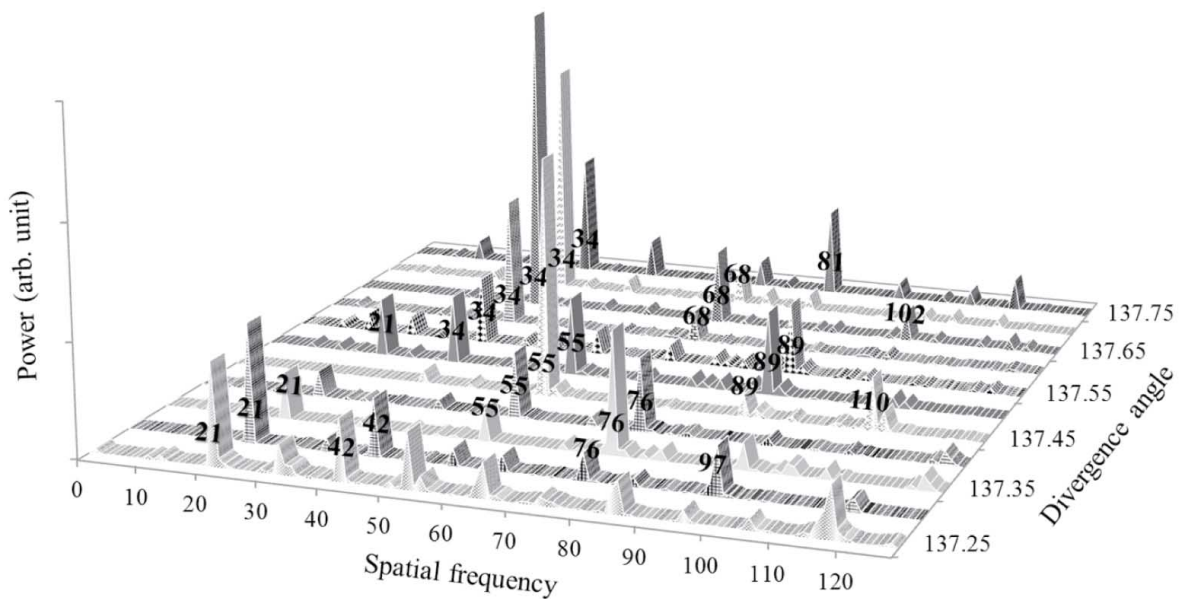


Fig. 12. Fourier transform results near the golden angle ϕ_τ in sunflower models with $n = 1000$ showing various parastichy numbers.

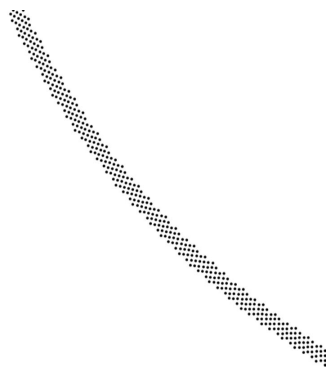


Fig. 13. One part of the simulated point pattern in the outer rim of a sunflower model with $p = 0.5$ and $\phi = \phi_\tau$.

monic waves seemed to appear as a characteristic feature of the Fourier transform. Conversely, Fig. 11(a) is the simulated point pattern for the case of $\phi = 137.55^\circ$, which was slightly greater than ϕ_τ . Figure 11(b) shows the Fourier transform result from the outer rim, and the large peaks were at 34 and 89. These numbers agreed with the parastichy numbers counted visually in the point pattern of Fig. 11(a) and were Fibonacci numbers.

Figure 12 shows the Fourier transform results of changing the angles from 137.25° to 137.75° in increments of 0.05° with $n = 1000$ and $p = 0.5$. Fourier peaks appeared at 21, 55, and 76 for a divergence angle of 137.35° . The numbers 21 and 55 were Fibonacci numbers; however, the number 76 was a Lucas number. The parastichy numbers were a mix of Fibonacci numbers and Lucas numbers. In addition, the spatial frequency of 97 was observed at a divergence angle of 137.30° . This number, 97, may belong to the generalized Fibonacci sequence $G(1, 4)$, judging from Table 1. Even for the slight angle change between 137.25° and 137.75° , spirals could be accurately counted and clas-

tions. Figure 10(b) shows the Fourier transform result from the outer rim, showing two large peaks at 55 and 110. The number 55 was a Fibonacci number, and the number 110 must have been the second harmonic wave of 55. Har-

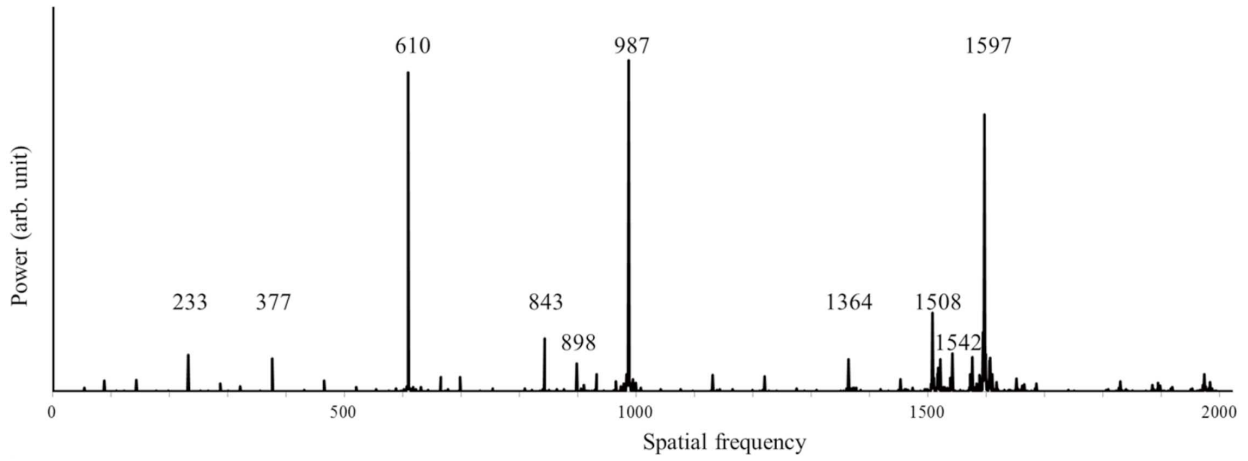


Fig. 14. Fourier transform result for $n = 100,000$, $p = 0.5$, and $\phi = \phi_r$.

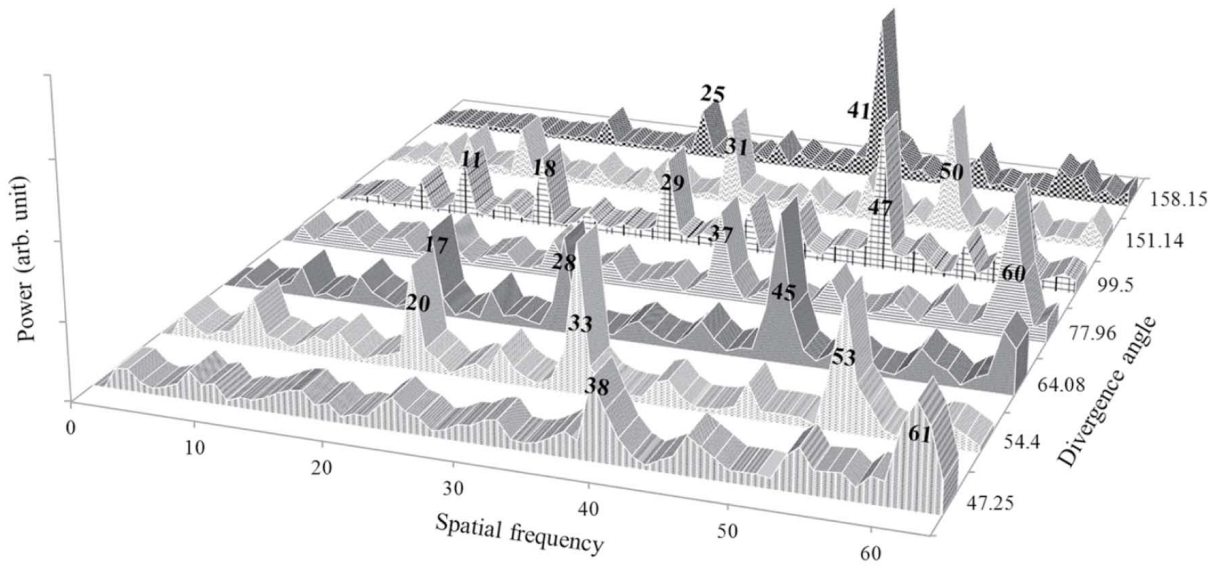


Fig. 15. Fourier transform results showing various spatial frequency (parastichy numbers) when the divergence angles are 47.25° , 54.40° , 64.08° , 77.96° , 99.50° , 151.14° , and 158.15° .

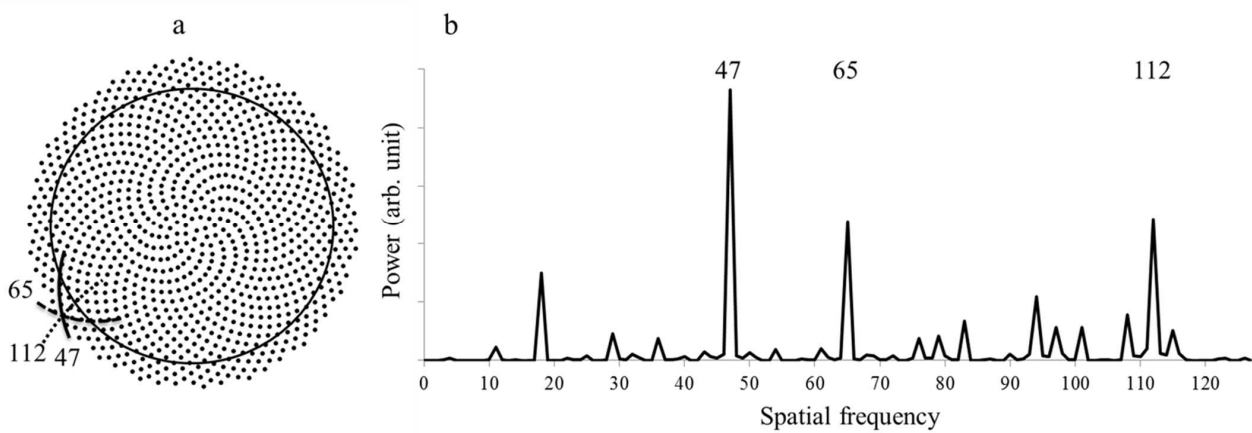


Fig. 16. (a) Simulated point pattern and (b) the Fourier transform result for a divergence angle of 99.65° for the region outside the black circle in panel (a).

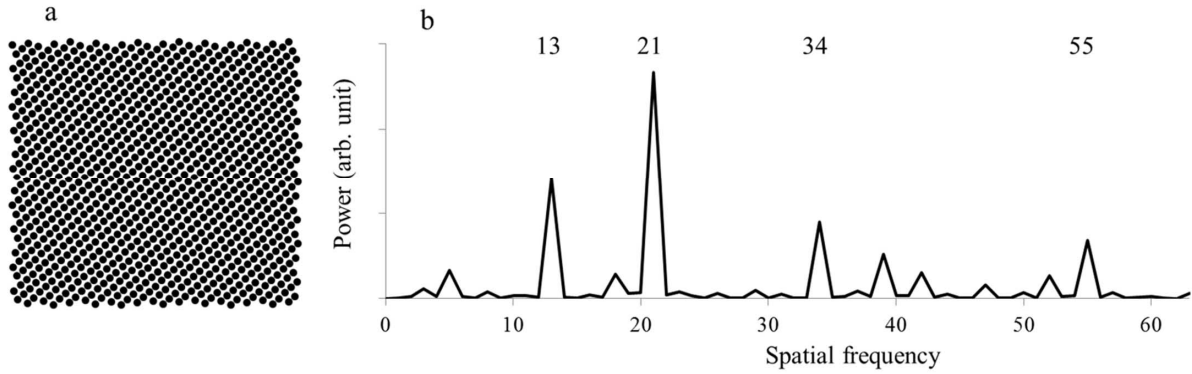


Fig. 17. (a) Simulated point pattern of a pineapple model with $n = 1000$, $p = 1$, and $\phi = \phi_\tau$. (b) The Fourier transform result for panel (a).

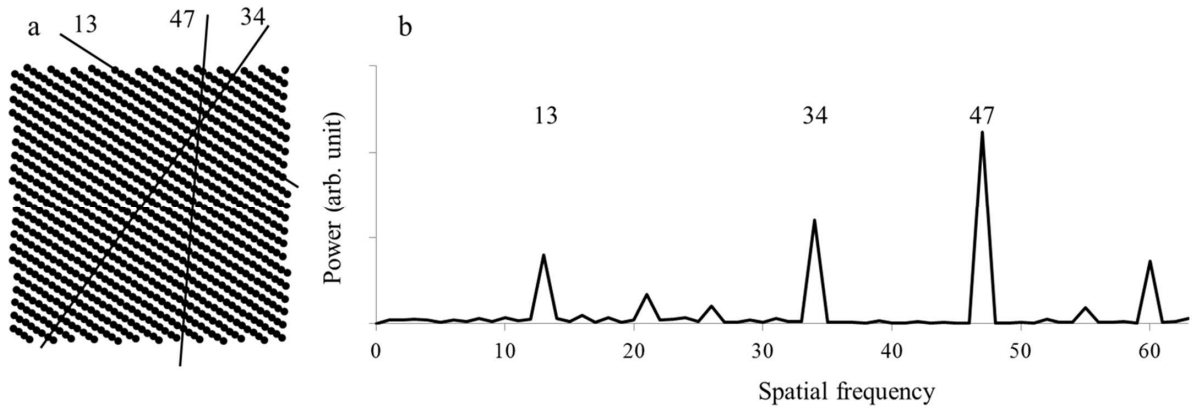


Fig. 18. (a) Simulated point pattern of a pineapple model with $n = 1000$, $p = 1$, and $\phi = 137.8^\circ$. (b) The Fourier transform result for panel (a).

sified by the parastichy numbers obtained via the presented Fourier transform method.

We also simulated a point pattern with $n = 100,000$, $p = 0.5$, and $\phi = \phi_\tau$ (Fig. 13). When parastichy numbers were visually counted from point patterns, there was a high probability of human counting errors due to the many packed points. We assigned the parastichy numbers using the Fourier transform method. The number of sample points for the Fourier transform was 4096 in the outer rim. Large Fourier peaks were observed at 610, 987, and 1597 (Fig. 14). These numbers corresponded to Fibonacci numbers. The results indicated that the presented method enabled us to measure large parastichy numbers using only a fraction of the point pattern.

4.2 Parastichy numbers for wide divergence angles in sunflower models

We investigated the effectiveness of the presented assignment method for various divergence angles as summarized in Table 1. We simulated the point patterns of sunflower models with divergence angles of 47.25° , 54.40° , 64.08° , 77.96° , 99.50° , 151.14° , and 158.15° . The parastichy numbers were measured using the discrete Fourier transform (Fig. 15). All the results agree with those in Table 1. When the divergence angle was 47.25° , large Fourier peaks appeared at 38 and 61. These numbers belonged to $G(1, 7)$. For 54.40° , Fourier peaks appeared at 20, 33, and 53. These

numbers were included in $G(1, 6)$. In addition, we examined the parastichy numbers for a divergence angle of 99.65° , which was slightly larger than the previously investigated divergence angle of 99.50° . Even though the angle difference between 99.50° and 99.65° was only 0.15° , the parastichy numbers could not be inferred from Adler's theorem. The simulated point pattern and the Fourier transform result are shown in Fig. 16(a). The visually counted parastichy numbers were 47, 65, and 112. The Fourier transform result in Fig. 16(b) reached the same numbers. This result suggested the effectiveness of the presented Fourier method, including arbitrary divergence angles that led to complex non-Fibonacci structures.

4.3 Parastichy numbers in pineapple models

We investigated the parastichy numbers for the pineapple model (see Subsec. 2.2) using the presented Fourier transform method. We simulated point patterns of the pineapple model with $n = 1000$ and $p = 1$ by changing the divergence angle. Figures 17(a) and 17(b) show the point pattern with $\phi = \phi_\tau$ and its Fourier transform result. Large Fourier peaks at 13, 21, 34, and 55 were observed, which corresponded to the Fibonacci sequence (see also Fig. 6). Therefore, parastichy numbers on curved surfaces such as the pineapple model could be found using the presented Fourier method. In the case of $\phi = 137.8^\circ$, the Fourier peaks of 13, 34, and 47 were observed in Fig. 18(b). The

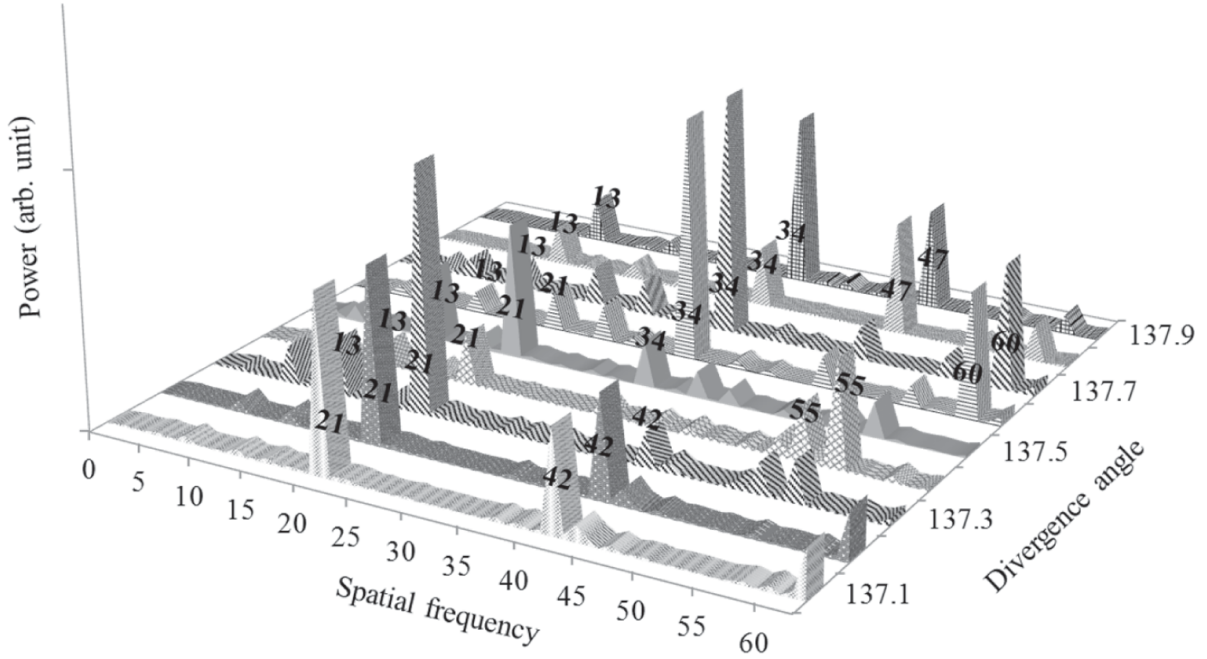


Fig. 19. Fourier transform results for pineapple models with several divergence angles ranging from 137.1° to 137.9° .

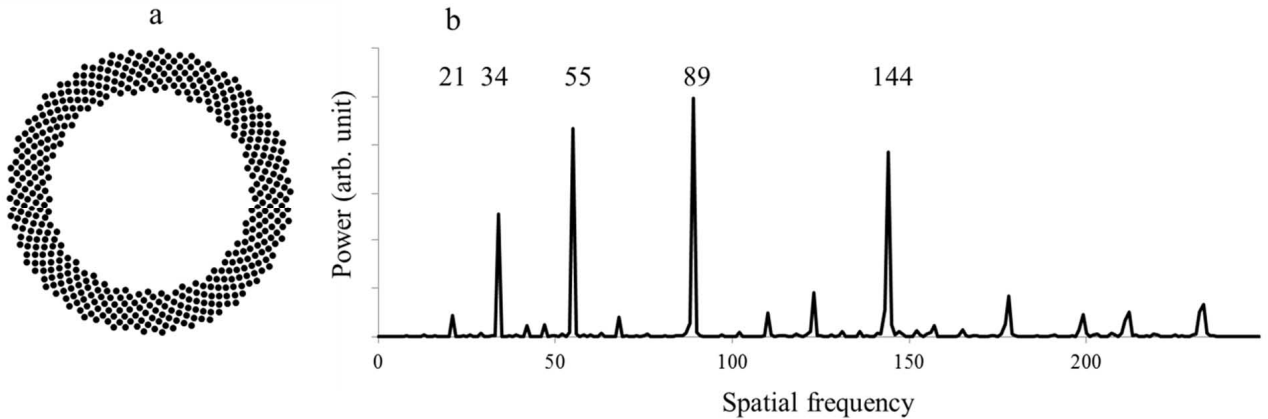


Fig. 20. (a) Simulated point pattern for a sunflower model with $n = 1000$, $p = 0.5$, $\phi = \phi_\tau$, and 499 sample points. (b) The Fourier transform result for panel (a).

number 47 was a Lucas number, so the parastichy numbers were a mix of Fibonacci and Lucas numbers. Figure 19 shows the Fourier transform results as the divergence angles were changed from 137.1° to 137.9° by increments of 0.1° . We recognized some transitions in the parastichy numbers. The transition from F_{21} to F_{34} occurred near $\phi = 137.4^\circ$, and L_{47} could be obtained for divergence angles greater than 137.8° .

4.4 Different sample point numbers

We examined the influence of the sample point number on the Fourier transform results. Figure 20(a) shows the simulated point pattern for a sunflower model with $n = 1000$, $p = 0.5$, $\phi = \phi_\tau$, and 499 sample points. Figure 20(b) shows the Fourier transform result. Several high Fourier peaks at 21, 34, 55, 89, and 144 could be observed. Compared to the result with 256 sample points in Fig. 9, we found that there was a remarkable match between them,

except for the power. Note that the sampling window in the radial direction was larger for the case with more sample points and more peaks appeared.

5. Summary

We showed that it is possible to directly measure parastichy numbers for point pattern simulations of sunflower models using one-dimensional discrete Fourier transforms. The detailed pattern analysis using the Fourier method revealed that the parastichy numbers in general cases were a mix of Fibonacci, Lucas, and generalized Fibonacci numbers. In addition, we demonstrated that it is possible to accurately assign parastichy numbers to curved surfaces such as those on a pineapple model. We believe that the presented method can be applied to extract the structural features of any spiral.

Acknowledgments. M.U. was supported by Grants-in-Aid for Scientific Research (B) (No. 26287066) and by a Grant-in-Aid for Challenging Exploratory Research (No. 15K13411) by the Ministry of Education, Culture, Sports, Science and Technology, Japan.

References

- Adler, I. (1974) A model of contact pressure in phyllotaxis, *J. Theor. Biol.*, **45**, 1–79.
- Adler, I., Barabe, D. and Jean, R. V. (1997) A history of the study of phyllotaxis, *Annals of Botany*, **80**, 231–244.
- Agrawal, A., Kejalakshmy, N., Chen, J., Rahman, B. M. A. and Grattan, K. T. V. (2008) Golden spiral photonic crystal fiber: polarization and dispersion properties, *Opt. Lett.*, **33**, 2716–2718.
- Authier, A. (2001) *Dynamical Theory of X-ray Diffraction*, Oxford University Press, New York, 73–78.
- Douady, S. and Couder, Y. (1992) Phyllotaxis as a physical self-organized growth process, *Phys. Rev. Lett.*, **68**, 2098–2100.
- Dunlap, R. A. (1997) *The Golden Ratio and Fibonacci Numbers*, World Scientific Publishing, New Jersey.
- Hofmeister, W. (1868) *Handbuch der Physiologischen Botanik*, Engelmann, 437–463.
- Jean, R. V. (2009) *Phyllotaxis*, Cambridge University Press, New York.
- Kikuta, S. (2011) *X-ray Scattering and Synchrotron Radiation Science-Fundamentals*, University of Tokyo Press, Tokyo, 144–148 (in Japanese).
- Koshy, T. (2001) *Fibonacci and Lucas Numbers with Applications*, John Wiley & Sons, Inc., New York, 109–115.
- Liew, S. F., Noh, H., Trevino, J., Negro, L. D. and Cao, H. (2011) Localized photonic bandedge modes and orbital angular momenta of light in a golden-angle spiral, *Opt. Express.*, **19**, 23631–23642.
- Mathai, A. M. and Davis, T. A. (1974) Constructing the sunflower head, *Math. Biosci.*, **20**, 117–133.
- Negishi, R. and Sekiguchi, K. (2007) Pixel-filling by using Fibonacci spiral, *Forma*, **22**, 207–215.
- Negro, L. D., Lawrence, N. and Trevino, J. (2012) Analytical light scattering and orbital angular momentum spectra of arbitrary Vogel spirals, *Opt. Express*, **20**, 18209–18223.
- Pennybacker, M. F., Shipman, P. D. and Newell, A. C. (2015) Phyllotaxis: Some progress, but a story far from over, *Physica D*, **306**, 48–81.
- Swinton, J., Ochu, E. and The MSI Turing’s Sunflower Consortium (2016) Novel Fibonacci and non-Fibonacci structure in the sunflower: results of a citizen science experiment, *The Royal Society Open Science*, **3**, 160091.
- Trevino, J., Cao, H. and Negro, L. D. (2008) Circularly symmetric light scattering from nanoplasmonic spirals, *Nano Letters*, **11**, 2008–2016.
- Turing, A. M. (1952) *Morphogen Theory of Phyllotaxis* (ed. Saunders, P. T., 1992, Collected Works of Turing, A. M.), Morphogenesis, North-Holland, Amsterdam.
- Turing, A. M. (1956) The Turing Digital Archive, <http://www.turingarchive.org>.
- Van der Linden, F. M. J. (1990) Creating phyllotaxis, the dislodgement model, *Math. Biosci.*, **100**, 161–199.
- Vogel, H. (1979) A better way to construct the sunflower head, *Math. Biosci.*, **44**, 179–189.